# THERMOMECHANICAL FINITE ELEMENT ANALYSIS OF STIFFENED, UNSYMMETRIC COMPOSITE PANELS WITH TWO DIMENSIONAL MODELS

Craig S. Collier, P.E. and Kevin A. Spoth
Lockheed Engineering and Sciences Co.
NASA Langley Research Center
Hampton, VA

Glenn C. Grassi
The MacNeal-Schwendler Corporation
Eastern Regional Office
Lake Ronkonkoma, New York

## ABSTRACT

A method is presented for formulating stiffness terms and thermal coefficients of stiffened, fiber-reinforced composite stiffened panels for input to finite element analysis (FEA). The method is robust enough to handle panels with general cross sectional shapes, including those which are unsymmetric or unbalanced. New thermal coefficients are introduced to quantify panel response from through-the-thickness temperature gradients. Equations are defined for stiffness, thermal expansion, and thermal bending that consider the full complement of membrane, bending, and membrane-bending coupling. A technique of implementing this capability with a single plane of shell finite elements using the MSC/NASTRAN™ FEA program is revealed. Thermomechanical analyses of an unsymmetric, hat-stiffened, metal matrix composite panel are shown to demonstrate the accuracy possible with planar, 2-D FEM's. 3-D FEA results are presented to verify the solutions. Ultimately, the significance of including this additional accuracy in smeared, equivalent plate 2-D models is proved with FEA of an aero-space plane.

# THERMOMECHANICAL FINITE ELEMENT ANALYSIS OF STIFFENED, UNSYMMETRIC COMPOSITE PANELS WITH TWO DIMENSIONAL MODELS

Craig S. Collier, P.E. and Kevin A. Spoth
Lockheed Engineering and Sciences Co.
NASA Langley Research Center
Hampton, VA

Glenn C. Grassi
The MacNeal-Schwendler Corporation
Eastern Regional Office
Lake Ronkonkoma, New York

## NOMENCLATURE

***laminate or panel***

| | |
|---|---|
| $\Delta T$ | In-plane temperature gradient |
| $\Delta G$ | Through-the-thickness temperature gradient |
| | *(i = 1, 2, 3)* |
| $h_i$ | Distance from the reference plane |
| $A_{ij}$, $B_{ij}$, $D_{ij}$ | Membrane, membrane-bending coupling, and bending stiffness terms |
| $A_i^{\alpha}$, $B_i^{\alpha}$, $D_i^{\alpha}$ | Membrane, membrane-bending coupling, and bending thermal force & moment coefs. |
| $NA_i^{\alpha}$, $NB_i^{\alpha}$, $ND_i^{\alpha}$ | MSC/NASTRAN FEA membrane, membrane-bending coupling, and bending thermal expansion & bending coefficients |
| | *(i = x, y, xy)* |
| $\alpha_i$, $\alpha_{ci}$ $\delta_i$, $\delta_{ci}$ | Thermal expansion, expansion coupling, bending, and bending coupling coefficients |
| $N_i$, $M_i$ | Forces and moments |
| $\epsilon_i$, $\kappa_i$ | Reference plane strains and curvatures |

***superscripts***

| | |
|---|---|
| p | Panel |
| T | Thermal |
| M | Mechanical |

## INTRODUCTION

Multidisciplinary conceptual design of high speed aircraft requires a quick structural analysis capability for vehicle optimization. High speed aircraft are often designed with stiffened panels fabricated from fiber-reinforced composite materials. The need for a quick analysis and the complexity of composite material, stiffened panels encourages approximations in the formulation of panel stiffness terms. The accuracy of composite stiffened panel formulation is further diminished for hot environments caused by supersonic flight. Temperature gradients induce forces and moments which must be quantified with thermal expansion and bending coefficients. Formulation of thermal coefficients is also complex, so they too are usually approximated.

This report highlights a method for accurately including composite lamina and laminate data in the formulation of stiffened panel structural properties. Thermal coefficients created to handle both in-plane and through-the-thickness temperature gradients are presented. This paper then shows how to input these data into the MSC/NASTRAN$^{TM}$ finite element analysis (FEA) program using a model with a single plane of finite elements.

### Stiffened Panels

Stiffened panels efficiently provide buckling stability. For a given unit weight, they can carry more service load than unstiffened plates or shells. Thermal forces and moments induced from temperature gradients are smaller for stiffened panels than they are for sandwich type panels, see Fig. 1. These qualities make them desirable for use as *hot* structure on high speed vehicles where weight reduction is a paramount objective.

Stiffened panels, however, are unsymmetric by nature of their shapes. Quantifying unsymmetric behavior is important because it significantly alters panel response. This effect may be a benefit when used to design lighter weight structure to satisfy a particular dominant load. Sandwich panels such as honeycomb become unsymmetric when designed to have different composite layups for the top and bottom facesheets.

Unsymmetric behavior causes coupling between membrane and bending panel response. Therefore bending will either shorten or lengthen the panel midplane. Likewise, a change in panel length will create curvature. This membrane-bending coupling is quantified in classical lamination theory [1,2] with the [B] stiffness matrix. If panel change in shape and size is due to a change in temperature, then corresponding thermal coupling coefficients noted as $\{B^{\alpha}\}$ must also be quantified. These coefficients and their ability to capture both in-plane and through-the-thickness temperature gradients, see Fig. 2, are introduced in references 3 and 4. The significance of including them for a detailed panel analyses and an entire aircraft analyses is reported in references 5 and 6 respectively.

Unsymmetric behavior is much more significant for stiffened panels than for laminates. Unsymmetric stiffened shapes produce coupling even when the panel is fabricated with conventional isotropic materials. A measure of the panel's membrane-bending coupling can be visualized in Fig. 3. The distance between the X-face and Y-face neutral axes can only be accommodated by the [B] and $\{B^{\alpha}\}$ data. Since the [B] and $\{B^{\alpha}\}$ data permit a common X-face and Y-face reference plane, the choice becomes available as to its location. Conventional lamination theory uses the midplane. However, any reference plane may be used such as the vehicle outer mold line or an offset to this to account for a thermal protection system.

Coupling data, as well as the membrane [A] & $\{A^{\alpha}\}$ and bending [D] & $\{D^{\alpha}\}$ stiffness terms and thermal coefficient data is calculated for the panel by extending the laminate formulations to the stiffened cross section, [3,4]. The technique is summarized in this paper.

## Finite Element Analysis

In-plane and through-the-thickness temperature gradients can be correctly applied and solved for anisotropic/orthotropic, unsymmetric, and unbalanced laminates or stiffened panels with a single plane of shell elements with the MSC/-NASTRAN FEA program. This is accomplished by including the full complement of smeared equivalent plate stiffness matrices and thermal expansion and bending coefficient vectors in the FEM data deck. Stiffness matrices for membrane, bending, and membrane-bending coupling are entered directly into MSC/NASTRAN with only minor adjustments as shown later. Thermal expansion and bending coefficient vectors for membrane, bending, and membrane-bending coupling cannot be entered into MSC/-NASTRAN without major adjustments to their formulation, [3,4]. A more thorough discussion is presented.

Smeared equivalent plate stiffness and thermal coefficient formulations of this paper are particularly useful for coarsely meshed models of a total structural entity such as an engine or airframe. Models of such large surface areas can only be accomplished with a single plane of shell finite elements. Too many elements would be necessary to construct a discrete three-dimensional model that defined the panel's stiffened shape. Fig. 4 depicts two models of the same fuselage surface area. It is apparent that many elements are needed to construct a three-dimensional model for the same panel area as accomplished with one element of a two-dimensional model. 3-D models are desirable because of their accuracy in capturing unsymmetric stiffness and through-the-thickness temperature gradients as proven with tests. A planar two-dimensional model can capture these same effects by including the complete set of panel thermal and stiffness properties in a shell finite element.

## Applications

The formulations of this paper apply to any stiffened panel concept, see Fig. 1, and are intended to be coded into computer application software. They are being added to the ST-SIZE structural-thermal sizing program [5] which is linked with MSC/NASTRAN to provide an analysis and sizing capability that can be iterated automatically until a structure's weight converges. These planar finite element models are well suited for achieving a multidisciplined design capability for high speed aircraft. A facility for storing and retrieving temperature and load dependent laminate data is necessary for optimization or sizing applications. The ST-SIZE program uses a material database.

The smeared equivalent plate models are also well suited to structural panel tests. The accurate techniques of this method provide a quick capability for calculating total panel stiffness that has laminates at varying temperatures. Such stiffnesses enable convenient correlation of test results to analytical predictions.

Limitations and assumptions of the method fall within those usually applied in classical lamination theory [4]. A primary assumption is that strain variation through the panel cross section follows the Kirchhoff hypothesis for laminated plates. This hypothesis maintains that a normal to the midplane remains straight and normal upon panel deformation and that stresses in the XY plane govern the laminate behavior. Implications of this hypothesis are: 1) membrane strains vary linearly through the panel cross section, 2) stresses vary in a discontinuous manner through the cross section, 3) the facesheet laminates are perfectly bonded to the coresheets, and 4) the bonds are infinitesimally thin and non-shear deformable. This implies that $\gamma^{p}_{xz}$, $\gamma^{p}_{yz}$, & $\epsilon^{p}_{z} = 0$, in addition to the usual *plane stress* assumptions of $\sigma_z$, $\tau_{xz}$, & $\tau_{yz} = 0$.

## STIFFNESS TERMS AND THERMAL EXPANSION & BENDING COEFFICIENTS

Panel stiffnesses and thermal coefficients are calculated by extending classical lamination theory to the stiffened cross section. Stacking sequence and lamina material properties are used to calculate orthotropic laminate properties. These laminate properties are treated as if they were individual laminae and used in extended classical lamination equations for calculating stiffened panel, orthotropic, or more general anisotropic properties. Special consideration is given to the actual shape of the stiffening member and its non-plate behavior. Fig. 5 illustrates the technique. The $h_i$ values of the laminate indicate distances of the plies from the mid-plane. For the stiffened panel, the $h_i$ indicate laminate distances from the midplane, or as depicted in this figure, from the outer mold line (OML).

FEM grid points are customarily located at a panel's midplane as depicted in the 2-D FEM of Fig. 4. Typically a structural analyst will choose the aerodynamically defined outer mold line (OML) as his FEM's surface. This causes the midplane of the structural surface to be in error; however, this is ordinarily done due to the difficulty of offsetting CAD generated lofted surfaces. This error causes an unconservative calculation of a structure's bending stiffness. While perhaps not significant for an airframe fuselage, this inaccuracy is substantial for wings and other shallow structural components. Another shortcoming of this approach, as displayed in Fig. 6, is that even though an analyst might go through the effort of offsetting his model properly, his offset is usually based on an assumed panel depth that is likely to change as strength and stability analyses are performed. A solution to these shortcomings is to always use the OML for the location of FEM grid points. Higher panel bending stiffnesses will be calculated this way but they will be balanced out with higher membrane-bending coupling stiffnesses. Note that a symmetric panel will now have non-zero membrane-bending coupling data.

Fig. 7 shows the force and moment sign convention used by both MSC/NASTRAN and the stiffness, thermal expansion, and thermal bending equations presented. Note that positive moment and curvature causes compression in the positive Z panel facesheet. This is a fundamental sign convention difference with classical lamination theory that defines positive moment and curvature as compression in the negative Z panel facesheet.

### Stiffness Formulation

Laminate: Laminate formulation can be summarized with the well known equations of membrane $A_{ij}$, membrane-bending coupling $B_{ij}$, and bending stiffness $D_{ij}$,

$$A_{ij} = \sum_{k=1}^{\eta} (\bar{Q}_{ij})_k \, (h_{k-1} - h_k) \qquad (1)$$

$$B_{ij} = -\frac{1}{2}\sum_{k=1}^{\eta} (\bar{Q}_{ij})_k \, (h_{k-1}^2 - h_k^2)$$

$$D_{ij} = \frac{1}{3}\sum_{k=1}^{\eta} (\bar{Q}_{ij})_k \, (h_{k-1}^3 - h_k^3)$$

These equations differ from others [1,2] because of the sign convention difference. The sign convention of Fig. 7 causes the usual terms $(h^i_k - h^i_{k-1})$ to become $(h^i_{k-1} - h^i_k)$ and the $B_{ij}$ to be negative. The rest of the laminate stiffness formulation is the same. Therefore, $\bar{Q}_{ij}$ are the transformed reduced laminae elasticities. $\bar{Q}_{ij} = Q_{ij}[T]^4$ where $[T]^4$ is a fourth order tensor and $Q_{ij}$ are the reduced laminae elasticities. As an example

$$Q_{11} = \frac{E_x}{(1 - \nu_{12}\nu_{21})} \qquad (2)$$

$Q_{ij}$ are interpolated from a material database using the laminate's temperature and compression or tension stress condition.

Panel: Laminate $A_{ij}$ from equation (1) are divided by their thicknesses to create new data entities $\bar{Q}^*_{ij}$ for use in temperature dependent and load dependent panel stiffnesses

$$A^p_{ij} = \left[ (\bar{Q}^*_{ij})_1 \, (h_0 - h_1) + (\bar{Q}^*_{ij})_3 \, (h_7 - h_8) \right] \qquad (3)$$

$$B^p_{ij} = -\frac{1}{2}\left[ (\bar{Q}^*_{ij})_1 \, (h_0^2 - h_1^2) + (\bar{Q}^*_{ij})_3 \, (h_7^2 - h_8^2) \right]$$

$$D^p_{ij} = \frac{1}{3}\left[ (\bar{Q}^*_{ij})_1 \, (h_0^3 - h_1^3) + (\bar{Q}^*_{ij})_3 \, (h_7^3 - h_8^3) \right]$$

The $h_i$ variables are illustrated in Fig. 5. By using the OML as the reference plane, they are: $h_0=0$, $h_1=-t_1$, $h_2=h_1-Nt_t$, $h_3=h_1-Nt_t/2$, $h_4=-H/2$, $h_8=-H$, $h_7=h_8+t_3$, $h_6=h_7+Nt_b$, and $h_5=h_7+Nt_b/2$. Also shown in Fig. 5 are the variables $t_1$, $t_2$, and $t_3$ which are the top facesheet, coresheet, and bottom facesheet thicknesses. $Nt_t$ and $Nt_b$ are the thicknesses of the coresheet top and bottom joining nodes. The subscripts 1, 2, and 3 on the $\bar{Q}^*_{ij}$ terms represent the different isotropic materials or composite layups. Properties of these materials or layups are based on their non-linear temperature and load dependent data. Equations for longitudinal stiffness terms $A^p_{11}$, $B^p_{11}$, and $D^p_{11}$ are expanded to account for additional geometric variables such as coresheet angle $\theta$, corrugation spacing $S_x$, and widths of the coresheet top and bottom joining nodes $Nw_t$ and $Nw_b$. As an example the equation for $B^p_{11}$ is

shown where these additional variables are shown in Fig. 5.

$$B_{11}^{p} = -\frac{1}{2}\left[(\bar{Q}_{11}^{*})_1\,(h_0^2-h_1^2) + \frac{(\bar{Q}_{11}^{*})_{2^t}\,(h_1^2-h_2^2)Nw_t}{S_x} + (\bar{Q}_{11}^{*})_3\,(h_7^2-h_8^2) + \frac{(\bar{Q}_{11}^{*})_{2^b}\,(h_6^2-h_7^2)Nw_b}{S_x} + \frac{2(\bar{Q}_{11}^{*})_2\,(h_3^2-h_4^2)t_2}{\sin\theta\ S_x} + \frac{2(\bar{Q}_{11}^{*})_2\,(h_4^2-h_5^2)t_2}{\sin\theta\ S_x}\right] \tag{4}$$

## MSC/NASTRAN Stiffness Terms

The full complement of either laminate or panel membrane [A], bending [D], and membrane-bending coupling [B] stiffness terms can be entered on MSC/NASTRAN MAT2 material bulk data cards. MSC/NASTRAN refers to all of the [A], [D], and [B] 3x3 stiffness terms as $G_{ij}$ [7]. $G_{ij}$ are the 11, 12, 13, 22, 23, and 33 fields of the MAT2 card. A MAT2 card is used for each stiffness behavior. Therefore, to model panel membrane, bending, and membrane-bending coupling stiffness requires three MAT2 cards. The MAT2 cards can represent laminates or smeared equivalent anisotropic plates. For simplicity, laminate nomenclature is used.

**Membrane stiffness terms:** MSC/NASTRAN adjusts the stiffness terms by factors located on the PSHELL property bulk data card. The thickness field on the PSHELL card can be any desired value. Sometimes the total panel height or facesheet thickness is used. If a value of 1.0 is used, then the entered values of membrane $G_{ij}$ will conveniently equal $A_{ij}$.

$$G_{ij} = \frac{A_{ij}}{\text{NASTRAN t}} \tag{5}$$

**Bending stiffness terms:** Bending stiffness terms are adjusted also by the thickness located on the PSHELL card. However, they are additionally adjusted by an inertia factor located on the PSHELL card. If the inertia factor is set to 12.0 and the thickness to 1.0, then the entered values of $G_{ij}$ will equal $D_{ij}$.

$$G_{ij} = \frac{12\,D_{ij}}{\text{NASTRAN } (t^3 \text{ x inertia factor})} \tag{6}$$

**Membrane-bending coupling stiffness terms:** Moment and curvature sign convention are different for MSC/NASTRAN and classical lamination theory. MSC/NASTRAN's convention shown in Fig. 7 causes the coupling $G_{ij}$ terms to be negative of classical lamination theory $B_{ij}$ terms. Since the formulation presented here uses the MSC/NASTRAN sign convention, coupling $G_{ij}$ are defined as

$$G_{ij} = \frac{B_{ij}}{\text{NASTRAN } t^2} \tag{7}$$

Again if the PSHELL thickness field is set to 1.0, then $G_{ij} = B_{ij}$.

## Thermal Coefficient Formulation

Thermal response of a laminate or a panel can be quantified with thermal coefficients and temperature gradients. Smeared equivalent plate thermal coefficients can be defined for the membrane, bending, and membrane-bending coupling response of a laminate or panel. Two unique temperature gradients can be identified such that their superposition captures each ply's temperature difference.

The first and more common gradient, see Fig. 2., is referred to informally as in-plane ($\Delta T$) which designates the laminate's or panel's change in temperature at a reference plane. (Strictly speaking, an in-plane gradient quantifies the temperature change on a surface. This data is captured by the FEM mesh.) The second gradient, called through-the-thickness ($\Delta G$), defines a linear variation of temperature through a laminate's depth or panel depth. Therefore, for a layer

$$t - t_0 = \Delta T + Z\Delta G \tag{8}$$

where Z is the measure of depth. The basic equation of thermal stress is

$$\sigma_i^{T} = Q_{ij}\,\alpha_i\,(t - t_0) \tag{9}$$

Equation (9) written in terms of thermal forces and moments for a homogenuous layer

$$\left(N_i^{T},\ M_i^{T}\right) = \int_{-h/2}^{h/2} \sigma_i^{T}\,(1,\ -Z)\,dz \tag{10}$$

can be written in terms of a laminate or panel by substituting equation (8) and (9) into equation (10).

$$\left(N_i^{T},\ M_i^{T}\right) = \int_{-h/2}^{h/2} \left(\bar{\Phi}_i\right)_k\,(\Delta T + Z\Delta G)\,(1,\ -Z)\,dz \tag{11}$$

where $\bar{\Phi}_i = \bar{Q}_{ij}\,\alpha_i$. By performing the integration and writing in matrix form, this equation is shown in reference

3 to equal

$$\begin{Bmatrix} N_i^T \\ M_i^T \end{Bmatrix} = \begin{bmatrix} A_{ij} & B_{ij} \\ B_{ij} & D_{ij} \end{bmatrix} \begin{Bmatrix} \alpha_i \Delta T - \delta_{ci} \Delta G \\ \alpha_{ci} \Delta T - \delta_i \Delta G \end{Bmatrix} \quad (12)$$

Equation (12) explicitly quantifies unsymmetric and unbalanced response caused by unsymmetric and unbalanced stiffness and by unsymmetric and unbalanced thermal expansion and bending. Reference 3 introduces twelve unique smeared equivalent plate membrane, bending, and membrane-bending coupling thermal coefficients: $\alpha_i$, $\alpha_{ci}$, $\delta_i$, and $\delta_{ci}$; to use with both in-plane and through-the-thickness temperature gradients to quantify thermal forces $\{N^T\}$ and thermal moments $\{M^T\}$. By lumping these coefficients together with their stiffness terms, equation (12) is reduced to

$$\begin{Bmatrix} N_i^T \\ M_i^T \end{Bmatrix} = \begin{bmatrix} A_i^\alpha & B_i^\alpha \\ B_i^\alpha & D_i^\alpha \end{bmatrix} \begin{Bmatrix} \Delta T \\ -\Delta G \end{Bmatrix} \quad (13)$$

by identifying thermal force $A_i^\alpha$, moment $D_i^\alpha$, and force-moment coupling $B_i^\alpha$ coefficients

$$A_i^\alpha = \sum_{k=1}^{\eta} (\bar{\Phi}_i)_k \, (h_{k-1} - h_k) \quad (14)$$

$$B_i^\alpha = -\frac{1}{2} \sum_{k=1}^{\eta} (\bar{\Phi}_i)_k \, (h_{k-1}^2 - h_k^2)$$

$$D_i^\alpha = \frac{1}{3} \sum_{k=1}^{\eta} (\bar{\Phi}_i)_k \, (h_{k-1}^3 - h_k^3)$$

Note the similarity of these to the formulation of the $A_{ij}$, $D_{ij}$, and $B_{ij}$ stiffness terms of equation (1). Other than the substitution of $Q_{ij}$ with $\bar{\Phi}_i$, the only other difference between the equations is the treatment of X & Y orthotropic coupling. Stiffness formulation defines separate terms to account for directional coupling via a 3x3 matrix. Thermal formulation defines orthotropic coupling at the lamina level and hence uses a 3x1 vector.

## MSC/NASTRAN Thermal Coefficients

MSC/NASTRAN documents their calculation of thermal behavior with the general equation

$$\begin{Bmatrix} \sigma_1 \\ \sigma_2 \\ \sigma_{12} \end{Bmatrix} = \begin{bmatrix} G_{11} & G_{12} & G_{13} \\ G_{21} & G_{22} & G_{23} \\ G_{31} & G_{32} & G_{33} \end{bmatrix} \left( \begin{Bmatrix} \epsilon_1 \\ \epsilon_2 \\ \gamma_{12} \end{Bmatrix} - (t - t_0) \begin{Bmatrix} A_1 \\ A_2 \\ A_{12} \end{Bmatrix} \right) \quad (15)$$

which relates stresses ($\sigma_i$) to strains ($\epsilon_i$) for an anisotropic homogenous layer. $G_{ij}$ are the $Q_{ij}$ reduced stiffness terms of equation (2). The $A_1$, $A_2$, and $A_{12}$ are the $\alpha_i$ expansion coefficients of the material. The term $(t - t_0)$ is its change in temperature. By rewriting with only thermal terms, equation (15) becomes

$$\sigma_i^T = Q_{ij} \, \alpha_i \, (t - t_0) \quad (16)$$

which is equation (9). For more general cases where the layer is not homogenouos, such as a composite laminate, or a panel, addtitional data becomes necessary. As previously noted, MSC/NASTRAN refers to the $A_{ij}$, $B_{ij}$, and $D_{ij}$ stiffness matrices as $G_{ij}$ and specifies a separate MAT2 card for each. The $A_1$, $A_2$, and $A_{12}$, coefficients also get entered for each MAT2. Likewise, when on separate MAT2 cards, they represent membrane, membrane-bending coupling, and bending thermal response. Unlike the stiffness terms, however, smeared equivalent plate thermal coefficients cannot be entered directly into MSC/NASTRAN. They must be formulated to account for MSC/NASTRAN's particular formulation of thermal forces and moments. MSC/NASTRAN computes thermal forces and moments by

$$N_i^T = A_{ij} \, NA_i^\alpha \Delta T - B_{ij} \, NB_i^\alpha \Delta G \quad (17)$$

$$M_i^T = B_{ij} \, NB_i^\alpha \Delta T - D_{ij} \, ND_i^\alpha \Delta G$$

where the stiffness matrices and thermal coefficient vectors shown can represent either a laminate or a stiffened panel. The $A_{ij}$, $B_{ij}$, and $D_{ij}$ stiffness matrices are input from equations (5, 6, & 7). The values for the smeared equivalent plate $NA_i^\alpha$, $NB_i^\alpha$, and $ND_i^\alpha$ thermal coefficients can be found by equating equation (17) to equation (13) and solving for $\Delta T$ and $\Delta G$ separately.

$$NA_i^\alpha = A_{ij}^{-1} A_i^\alpha \quad (18)$$

$$NB_i^\alpha = B_{ij}^{-1} B_i^\alpha$$

$$ND_i^\alpha = D_{ij}^{-1} D_i^\alpha$$

Because equation (17) does not join thermal force calculation with moment calculation, as does equations (12 & 13), the ensuing stiffness matrices of equation (18) are inverted separately as 3x3 matrices. $B^{ij}$ must not be singular.

A change in the panel's bulk temperature is entered in the FEA by supplying the reference temperature on the MAT2 record and the loadcase dependent temperature on the TEMPP1 record. The effect of in-plane temperature gradients is then captured with the model's discretization. Loadcase dependent through-the-thickness gradients are entered on an element basis with the TEMPP1 record. When the MSC/NASTRAN thickness and inertia factor are set to 1.0 and 12.0 respectively, then the load case depen-

dent temperature gradients can be entered directly.

## LOAD DEPENDENT RESIDUAL STRAINS

Residual panel strains and stresses caused by thermal growth are resolved on a laminate basis for each loadcase. They develop in stiffened panels when the panel laminates want to elongate non-uniformly when heated. Because the panel laminates cannot act independently, they develop residual strains and stresses when forced to strain together as a unit of the panel. Panel curvature dictates that all laminate strains follow its through-the-depth strain profile. This profile is linear due to Kirchoff's hypothesis that a normal to the midplane remains straight and normal upon panel deformation. The residual strain is the difference between the strain that occurs in the laminate when made a segment of the stiffened panel's linear strain profile, and the strain that occurs in the laminate when allowed to thermally grow unattached to the panel.

2-D FEA is able to use smeared equivalent plate properties for a stiffened panel because of this "plane sections remain plane" hypothesis. In principle, during FEA, panel laminates strain together as a unit providing a linear strain profile through-the-depth, and thus do not include residuals. In order to quantify a laminate's "design-to" strains (or its ply strains and stresses by using its constitutive matrices), its residual strains must also be quantified and added to FEA computed strains, see reference 3.

## TYPICAL STIFFENED PANEL ANALYSES

The fuselage and wing skins of high speed vehicles are commonly designed with stiffened panels. A hat stiffened, fiber-reinforced, metal matrix composite panel, see Fig. 8., is used in this paper for comparative analyses. Metal matrix composites are chosen for their high temperature capability, some having a service use up to 1300°F. When allowing a stiffened panel to reach these high temperatures, its large membrane, bending, and membrane-bending coupling thermal response must be analytically quantified.

Thermomechanical finite element analyses were performed using different modeling strategies. Results are shown for a finely meshed, discrete 3-D model; a 2-D unsymmetric model that uses this formulation; and a 2-D symmetric model that uses conventional approximate formulations. Significant differences between 2-D equivalent plate formulations are demonstrated for FEA of a hypersonic aero-space plane that uses this typical panel design.

### Panel Design and Temperatures

The panel cross section shape, dimensions, and laminate layups are those which are commonly produced by structural sizing optimization codes. The hat shape is fabricated by brazing the facesheet to the corrugated coresheet. Shown to the left of the section in Fig. 8. is the temperature profile which is typical of those analyzed for high speed flight. The panel's midplane temperature is 625°F. while its hottest point is on top of the facesheet (850°F.) and its coldest point is on the bottom of the coresheet (400°F.). These laminate temperatures are well within the material's limit. The shaded rectangle represents a uniform in-plane gradient of 555°F (625°F-70°F). The double shaded triangles represent a through-the-thickness gradient of 300°F/in. By superimposing the two gradients, the variation of temperature through the panel's depth is known, as illustrated with the bold line. The facesheet's average temperature of 842.5°F. and the coresheet's average temperatures of 832.75°F., 617.5°F., and 402.25°F. are used for interpolating a material database. Laminate material properties are also retrieved from the database according to compression or tension stress conditions. Compression elasticities of metal matrix composites are approximately 35% higher than their tension elasticities at elevated temperatures. These load and temperature dependent laminate data are used for formulating panel stiffness terms and thermal coefficients.

### Panel Data

The typical corrugated stiffened panel has the following properties when this general anisotropic formulation is used. The equivalent orthotropic plate data shows the "13" and "23" terms of the stiffness matrices and the "3" terms of the MSC/NASTRAN thermal coefficient vectors to be zero because the laminates are balanced. If the laminates were not balanced,

$$A^p_{ij} = \begin{bmatrix} 1400599 & 259740 & 0.0 \\ 259740 & 697134 & 0.0 \\ 0.0 & 0.0 & 201010 \end{bmatrix}$$

$$B^p_{ij} = \begin{bmatrix} -549085 & -188311 & 0.0 \\ -188311 & -505422 & 0.0 \\ 0.0 & 0.0 & -145732 \end{bmatrix}$$

$$D^p_{ij} = \begin{bmatrix} 595340 & 136580 & 0.0 \\ 136580 & 366577 & 0.0 \\ 0.0 & 0.0 & 105698 \end{bmatrix}$$

The hat panel stiffness terms.

$$NA^{p\alpha}_i = \begin{Bmatrix} 3.8554 \\ 4.5463 \\ 0.0 \end{Bmatrix} \quad NB^{p\alpha}_i = \begin{Bmatrix} 4.0632 \\ 4.4689 \\ 0.0 \end{Bmatrix} \quad ND^{p\alpha}_i = \begin{Bmatrix} 3.8887 \\ 4.5339 \\ 0.0 \end{Bmatrix}$$

The hat panel MSC/NASTRAN thermal coefficients ($10^{-6}$).

or if an off axis reference direction was used for the panel, these terms would not be zero and fully populated, equivalent plate, anisotropic data would have been produced. The midplane was used as the reference plane in lieu of the OML for ease of comparison to traditional methods which use neutral axes as reference planes. Note the relatively large membrane-bending coupling $B_{ij}$ terms and that all of the thermal coefficients are different values which indicates the significance of the unsymmetric nature of the panel. The highest thermal coefficient is $4.5^{-6}$ (in-F°/in), less than values of typical metallic materials. Consequently, the behavior of this panel with isotropic, metallic materials would be similar, yet amplified.

## Thermomechanical Panel Analyses

Thermal forces, moments, strains, and curvatures were computed to compare results of different analysis methods. The best possible structural-thermal analysis was performed to arrive at baseline results. Baseline strains, curvatures, forces, and moments were acquired by rigorous analysis of each of the panel's laminates which included executing classical lamination codes. Each laminate's thermal response was used to assemble the panel's response maintaining the equilibrium of forces and moments and the simultaneous compatibility of the six strain and curvature degrees of freedom of the panel.

3-D FEA of the panel was performed to provide a check of the baseline results. A finely meshed model consisting of 9600 MSC/NASTRAN CQUAD4 shell elements, similar to the 3-D FEM portrayed in Fig. 4. was built and executed. Since elements were included to model the coresheet corrugation pattern, the unsymmetric nature of the panel was captured. Each element used temperature dependent laminate stiffnesses [A] & [D] and thermal coefficients $\{A^{\alpha}\}$ & $\{D^{\alpha}\}$ generated by classical lamination codes. This data was input without modification directly into the MAT2 material data cards.

Two different types of 2-D FEA were performed for the panel. The first type used this formulation and is later referred to as the unsymmetric 2-D FEA. The other analysis uses traditional stiffened panel formulation and is referred to as the symmetric 2-D FEA because it ignores unsymmetric behavior. The only difference between these models is the stiffness and thermal coefficient input data. All other model data is identical. These models are different from the 3-D FEM in that they have smeared equivalent plate properties and do not have elements that model the coresheet corrugation. However the mesh density (3200 elements) and connectivity of the facesheet surface is the same.

Two different panel boundary conditions are analyzed. The first condition prevents the panel from straining or curving upon applied temperature loads. This condition may be visualized as restraining the panel's growth within rigid walls. Consequently the full magnitude of induced thermal forces and moments develop, Table 1. The second boundary condition allows full thermal growth by constraining the panel in the FEM only at the center grid to prevent rigid body motion. Thermal forces and moments are zero for this case, Fig. 9. These two boundary condition cases are the extremes of in-service possibilities and therefore band the level of accuracy expected for actual conditions.

*Table 1 Comparison of computed panel forces and moments to both temperature gradients.*

| | Baseline results | 2-D FEA Unsymm. | 3-D FEA | 2-D FEA Symm. |
|---|---|---|---|---|
| Nx | -4574 | -4574 | -4595 | -3652 |
| Ny | -3222 | -3222 | -3223 | -2315 |
| Mx | 2586 | 2586 | 2581 | 1891 |
| My | 2336 | 2336 | 2337 | 1678 |

The exact match between 2-D unsymmetric FEA computed forces and moments and the baseline results is not surprising. This happens because the constrained boundary conditions (rigid walls) do not allow the element shape functions to come into play. The agreement is actually a substantiation of the defined MSC/NASTRAN force and moment equations (17) and thermal coefficients (18). The second boundary condition where growth is permitted is more of a measure of the 2-D FEM's ability to capture the panel's unsymmetric behavior. In some respects, the good agreement to the 3-D FEM's double curvature deformed shape, Fig. 9, gives credence to the Kirchoff hypothesis of plane sections remain plane and linear strain distribution through plate thickness (in this case panel depth) as implemented with the smeared equivalent plate approach. The agreement also confirms the application of this formulation to unsymmetric stiffened composite panels and the facility to capture both the in-plane and through-the-thickness temperature gradients with the expansion, bending, and expansion-bending coupling thermal coefficients. Because symmetric 2-D FEA omits this additional data, its deformed shape exhibits erroneous curvature.

Symmetric 2-D FEA of traditional methods significantly under predicts both mechanical and thermal panel response. This is due to dissimilarities in the formulations of panel stiffness terms and thermal coefficients. Traditional formulations currently being practiced require treating each layup type with different approximations, calculating neutral axes, effective thicknesses, effective areas (EA), effective moment-of-inertias (EI), effective elasticities, etc. in both the X and Y directions separately using modular ratios and the parallel axis theorem; thus treating the panel as two detached perpendicular beams. Doing this omits panel

strain compatibility because the X-face unit width section is not coupled with the Y-face unit width section. Attempts to couple the directions would be in error since the X-face neutral axis does not lay on the Y-face neutral axis. Finally, membrane-bending coupling of unsymmetric stiffness, $[B^p]$, and the membrane-bending coupling of unsymmetric thermal expansion and bending, $\{B^{p\alpha}\}$ are missing.

In order to get the most accurate solution with the 2-D symmetric FEA, the FEM input data included X & Y plate coupling as produced by the 3x3 membrane and bending stiffness matrices and in the six expansion and bending thermal coefficients. The 2-D symmetric FEM also contained the through-the-thickness gradient. This FEA, although, was not able to include load dependent residual strains.

The reported moments of Table 1 are those values found at the panel midplane. Unlike forces, the magnitude of moments vary according to the location of their reference planes. Traditional symmetric analysis uses the neutral axes for reporting moment. Accordingly, at the X-face neutral axis $M_x = 792$ and at the Y-face neutral axis $M_y = 0.0$. However, moments have limited usefulness at the neutral axes because they cannot be coupled.

The unsymmetric 2-D FEA actually compares better to the baseline results than the 3-D FEA. This could be caused by an innate shortcoming of the 3-D FEM which is due to the top segment of the coresheet and the facesheet being modeled as if they lay on the same plane. The actual separation between them is equal to $t_1/2 + Nt_l/2$, see Fig. 5. This distance is not contained in the 3-D FEM because the same grid points are needed for connecting the coresheet elements to the facesheet elements. After making minor adjustments to account for the top of the coresheet being modeled on the same plane as the facesheet, the 3-D FEM produces nearly the same results as the baseline. However, the 32" square hat panel requires at least 2240 elements in order to capture the corrugated shape of the coresheet, (one element is needed to span the panel depth). With 2240 elements, thermal $M_x$ has a -2.8% error. By using an equivalent plate 2-D FEM, only one element is needed for the 32" panel while still maintaining 0% error.

**Thermomechanical Vehicle Analyse3s**

Presented are results for a hypersonic aero-space plane that has been analyzed to mach 10 in-plane and through-the-thickness temperature gradients. Shown are the mach 10 thermal forces, Fig. 10a, and moments, Fig. 10b, computed with the cross section size and layup of Fig. 8. Differences between correct unsymmetric analysis and incorrect traditional symmetric analysis, as documented in Table 1 for a panel analysis, also occur for a total vehicle analysis. Illustrated are the FEA solved thermal force and moment gradients of the two equivalent plate formulations. Although not shown, comparable differences occur for computed mechanical forces and moments.

## CONCLUSIONS

The techniques presented in this paper provide the capability to model stiffened composite panels of any geometric cross sectional shape with a single plane of shell finite elements. Formulations are defined which enable the solution to any applied thermomechanical load combination. This capability comes from: (1) defining explicit MSC/NASTRAN thermal coefficients of membrane, bending, and membrane-bending coupling for both in-plane and through-the-thickness temperature gradients, and (2) including temperature dependent, load dependent, non-linear material data in the constitutive, smeared equivalent plate representation of either laminates or stiffened panels.

A major benefit of being able to accurately formulate stiffened panels with smeared equivalent plate properties is that a coarsely meshed 2-D FEM with a single plane of shell finite elements can be used to analyze complex thermomechanically loaded structures. Traditional methods of formulating equivalent plate panel stiffness and thermal coefficients, though intuitive, are difficult to use for a wide possibility of applications. More importantly they give incorrect results as demonstrated. 2-D FEA that uses this formulation correlates very well with 3-D FEA.

## ACKNOWLEDGEMENTS

This work was performed for the Systems Analysis Office/National Aero-Space Plane Office under NASA contract NAS1-19000 at Langley Research Center in Hampton, Virginia.

## REFERENCES

[1] Jones,R.M., *Mechanics of Composite Materials*, Hemisphere Publishing Corporation, Washington, DC, 1975

[2] Halpin,J.C., *Primer on Composite Materials: Analysis*, Technomic Publishing Company, Inc., Lancaster, PA, 1984

[3] Collier, C.S., "Stiffness, Thermal Expansion, and Thermal Bending Formulation of Stiffened, Fiber-Reinforced Composite Panels", AIAA/ASME/ASCE/AHS/ACS 34th Structures, Dynamics, & Materials Conference, La Jolla, CA, April 19-22, 1993, Paper No. AIAA-93-1569

[4] Collier, C.S., *COMPOSITE STIFFENED PANELS: Part 1 - Stiffness, Thermal Expansion, and Thermal Bending Formulation for Finite Element Analysis*, NASP CR 1134, April 1992

[5] Collier, C.S., "Structural Analysis and Sizing of Stiffened, Metal Matrix Composite Panels for Hypersonic Vehicles", AIAA 4th International Aerospace Planes Conference, Orlando, FL, December 1-4, 1992, Paper No. AIAA-92-5015

[6] Collier, C.S., "A General Method for Structural Analysis and Sizing of Composite Stiffened Panels Using 2-D Finite Element Models", NASP Technology Review, Monterey, CA, April 21-24, 1992, Paper No. 212

[7] The MacNeal-Schwendler Corporation, *MSC/NASTRAN User's Manual*, Vol 1, Version 67, The MacNeal-Schwendler Corporation, Los Angeles, CA, Aug. 1991

## TRADEMARKS

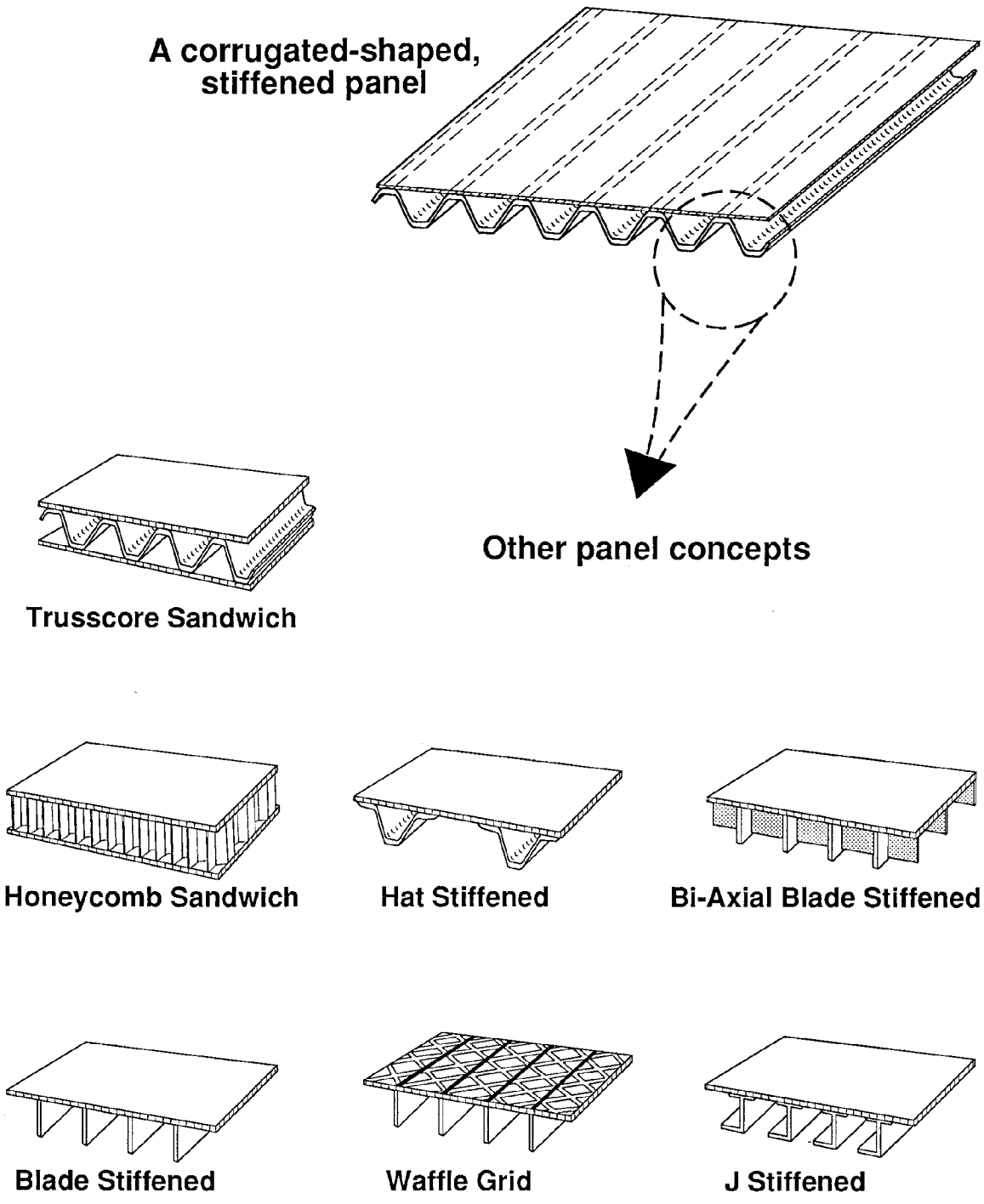


*Figure 1 2-D FEM's can accurately model any panel concept.*

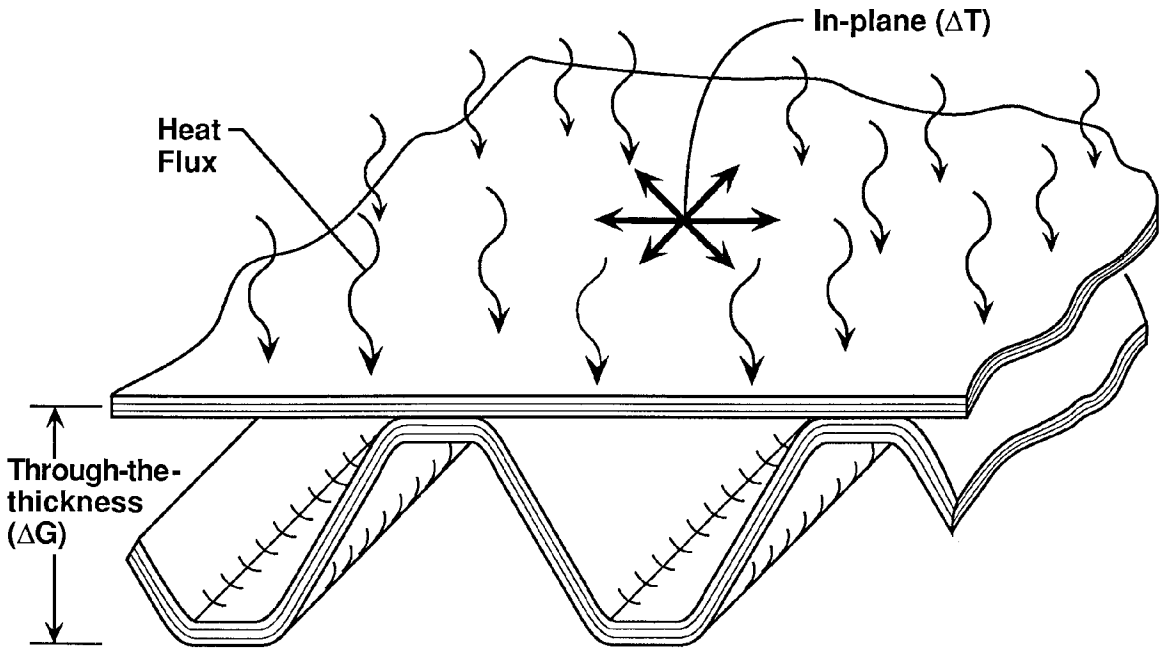


*Figure 2 Aerodynamic heating of high-speed aircraft produces two kinds of temperature gradients.*

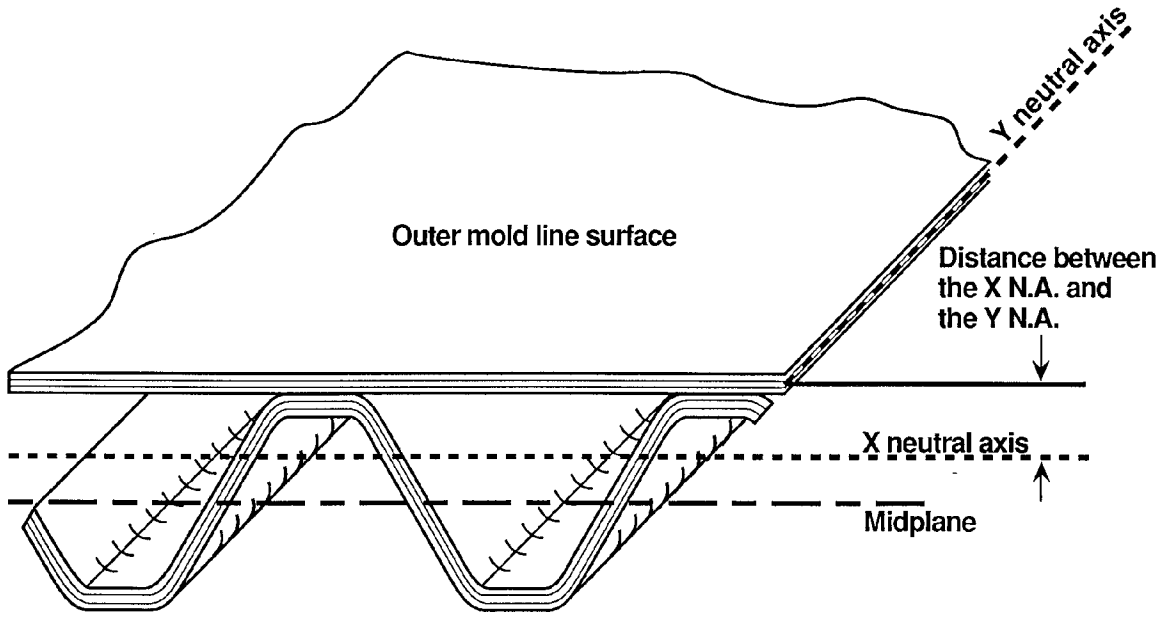


*Figure 3 Any reference plane may be used to calculate properties by including unsymmetric data.*

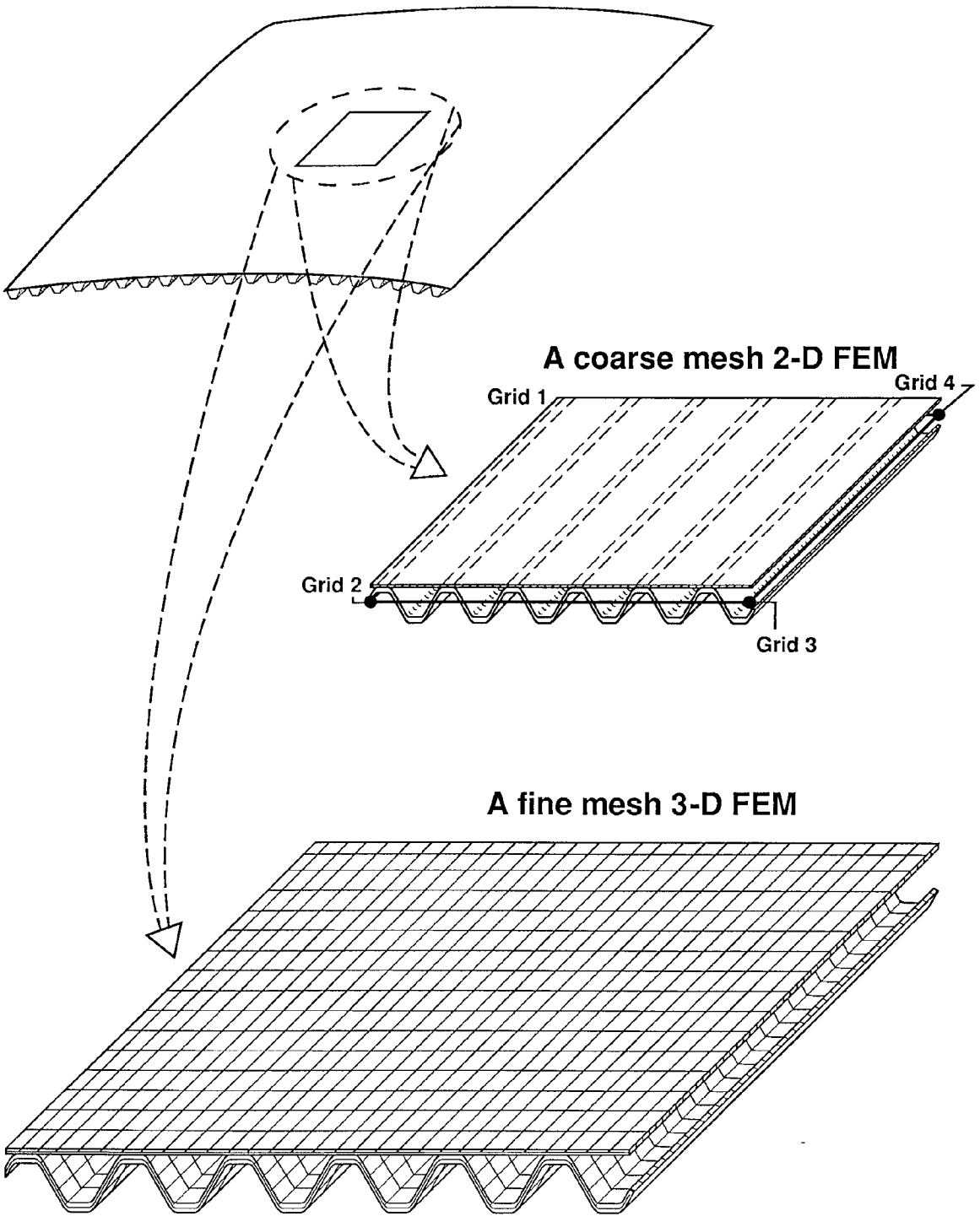


*Figure 4 Accurate results are possible with 2-D planar FEM's.*

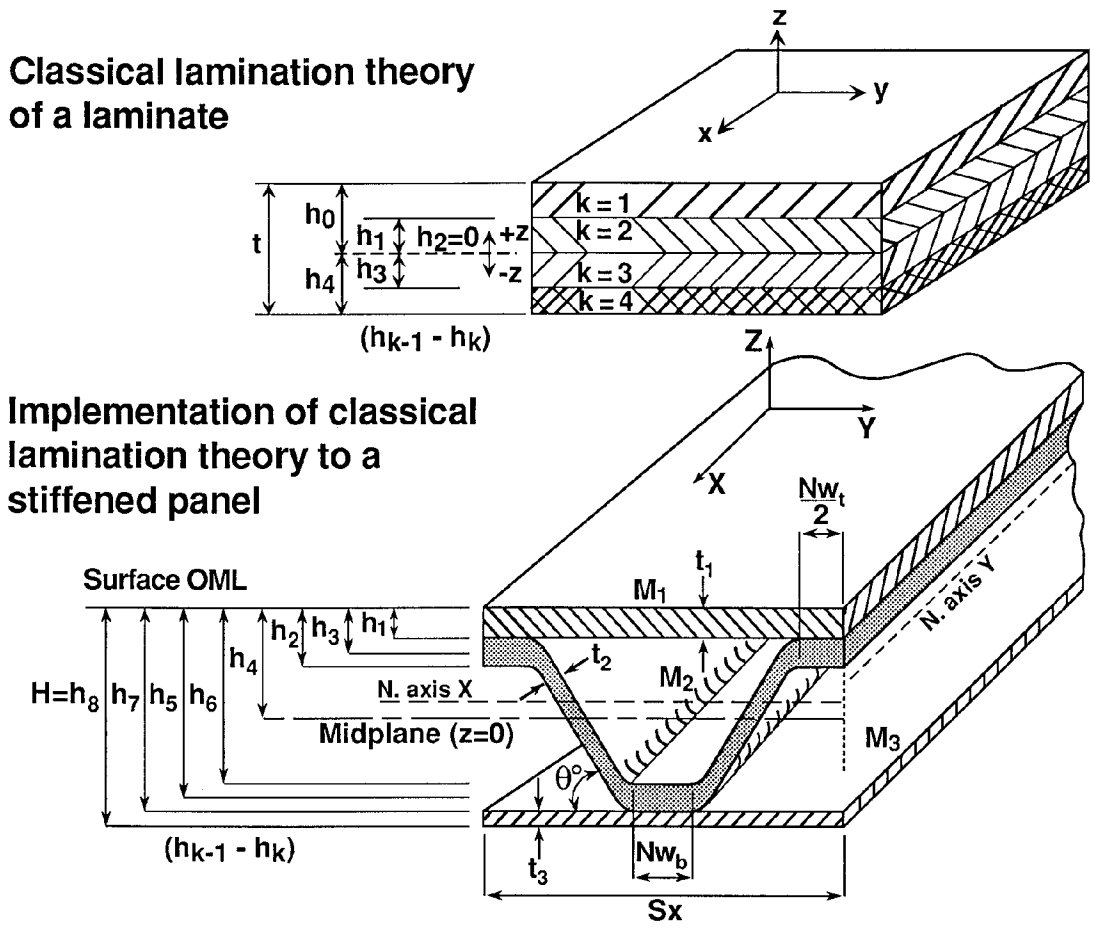


*Figure 5 Laminate formulation is extended to stiffened panels.*

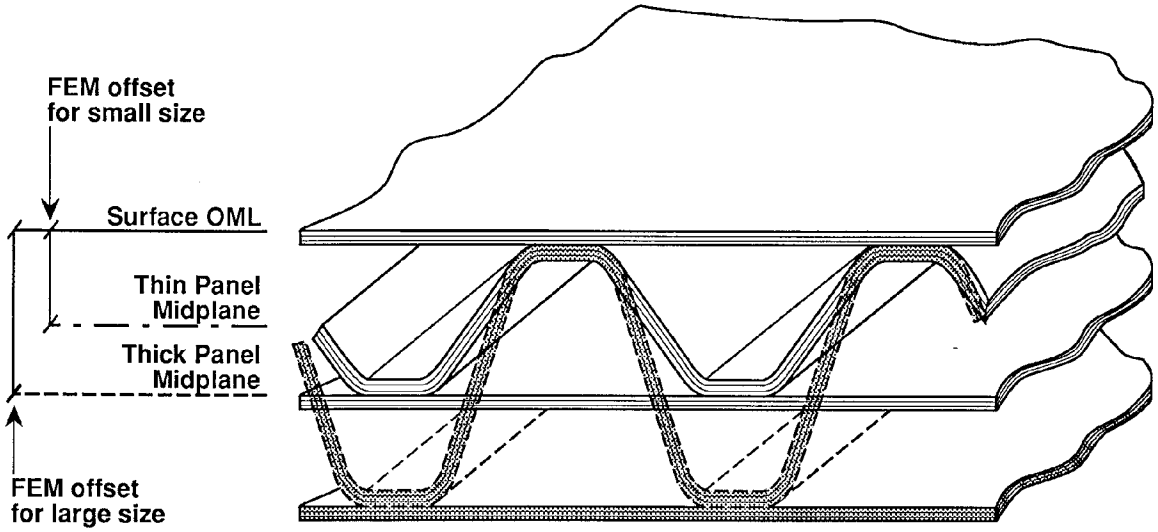


*Figure 6 The best choice of a FEM reference plane is the surface outer mold line.*

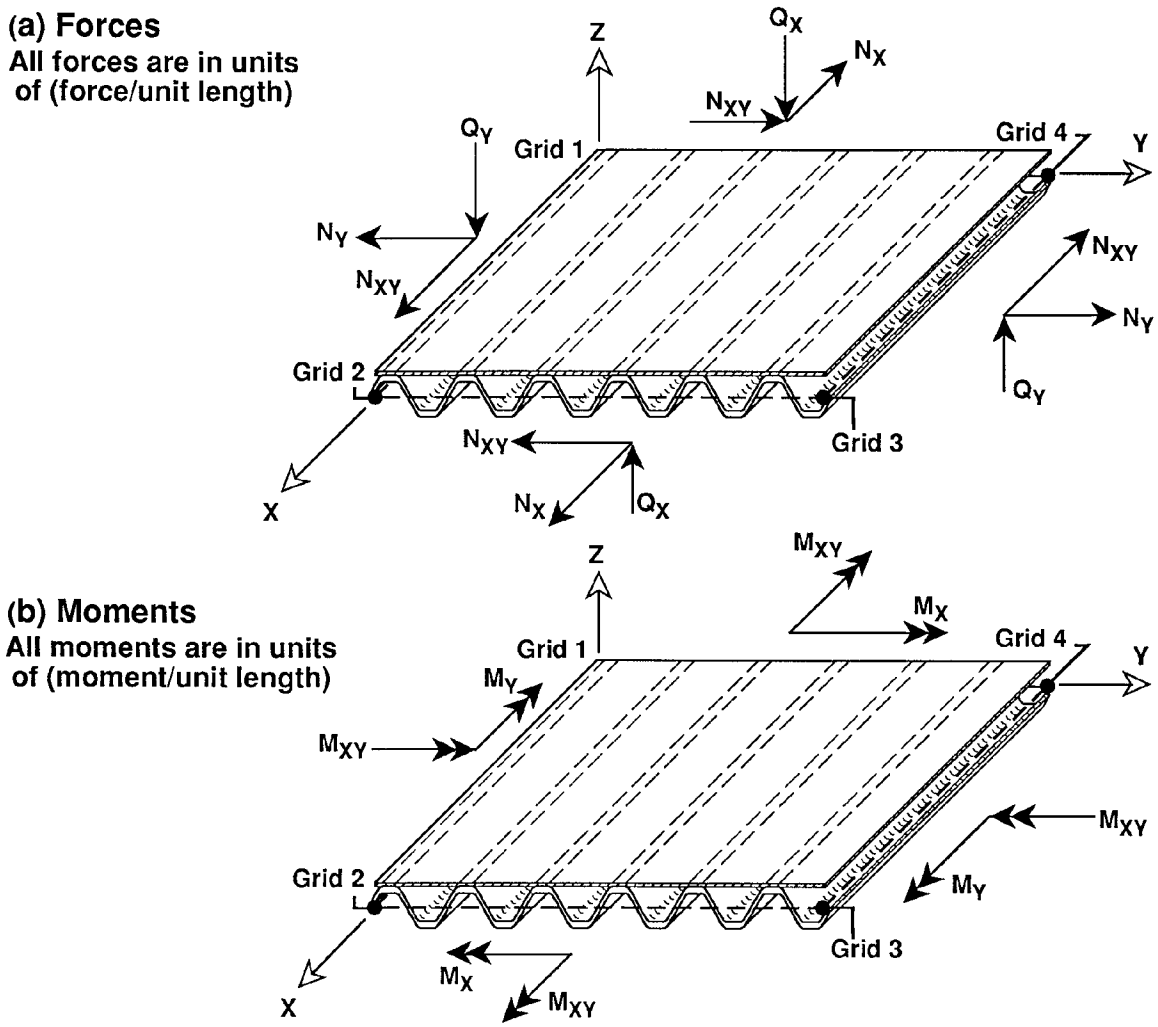


*Figure 7 Panel and finite element positive sign convention.*

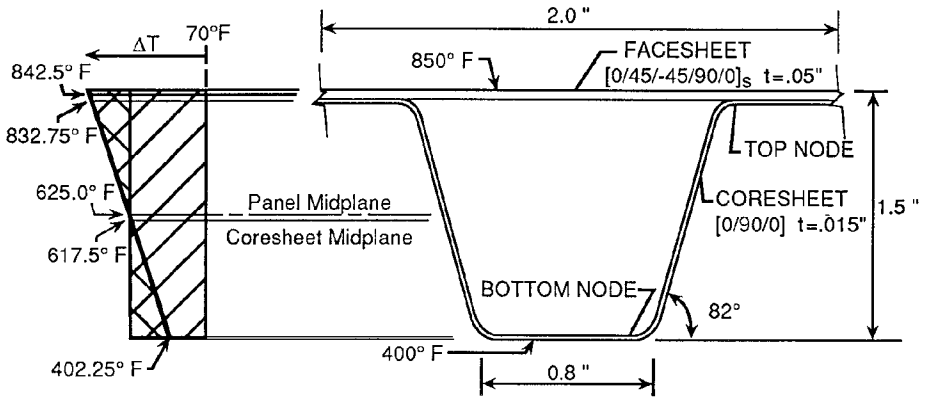


*Figure 8 Typical hat stiffened panel and temperature profile.*

# FEM DEFORMED PLOTS OF THE PANEL RESPONSE TO A UNIFORM TEMPERATURE INCREASE OF 555 F. (IN-PLANE GRADIENT ONLY)

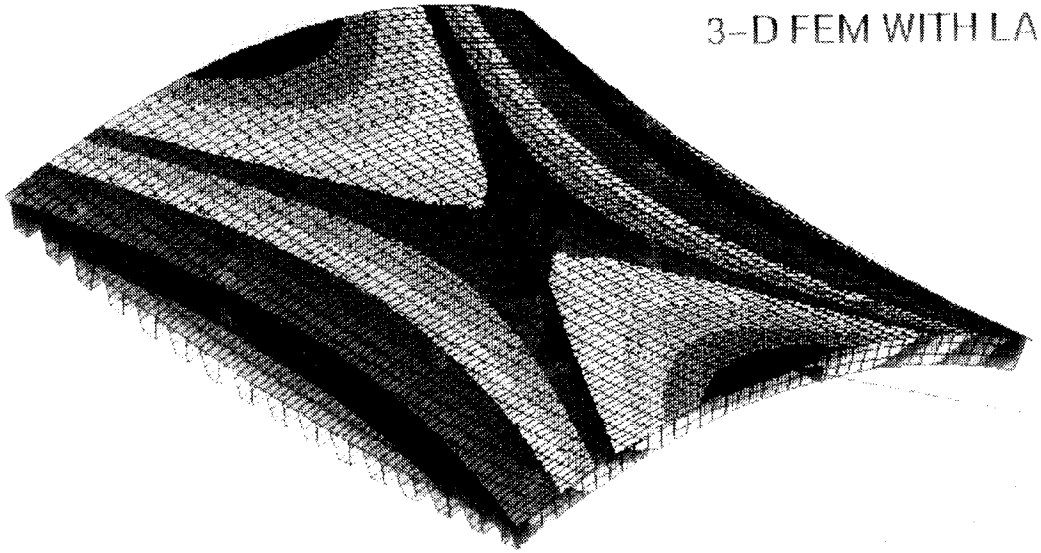


THE DEFORMED SHAPES ARE IDENTICAL

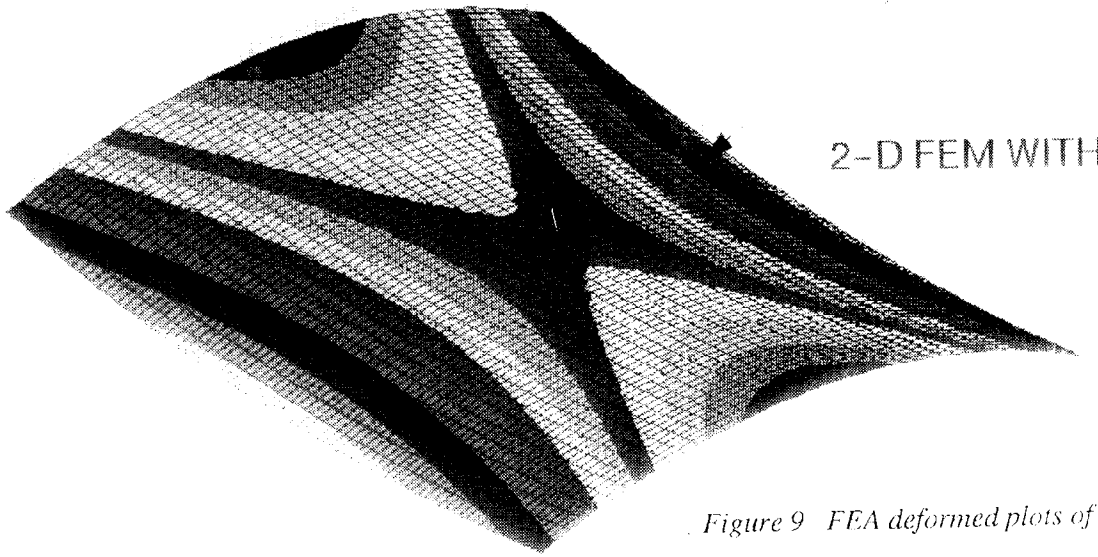


CORRECT ANALYSES SHOWS THE PANEL IN DOUBLE CURVATURE

*Figure 9 FEA deformed plots of the panel response.*

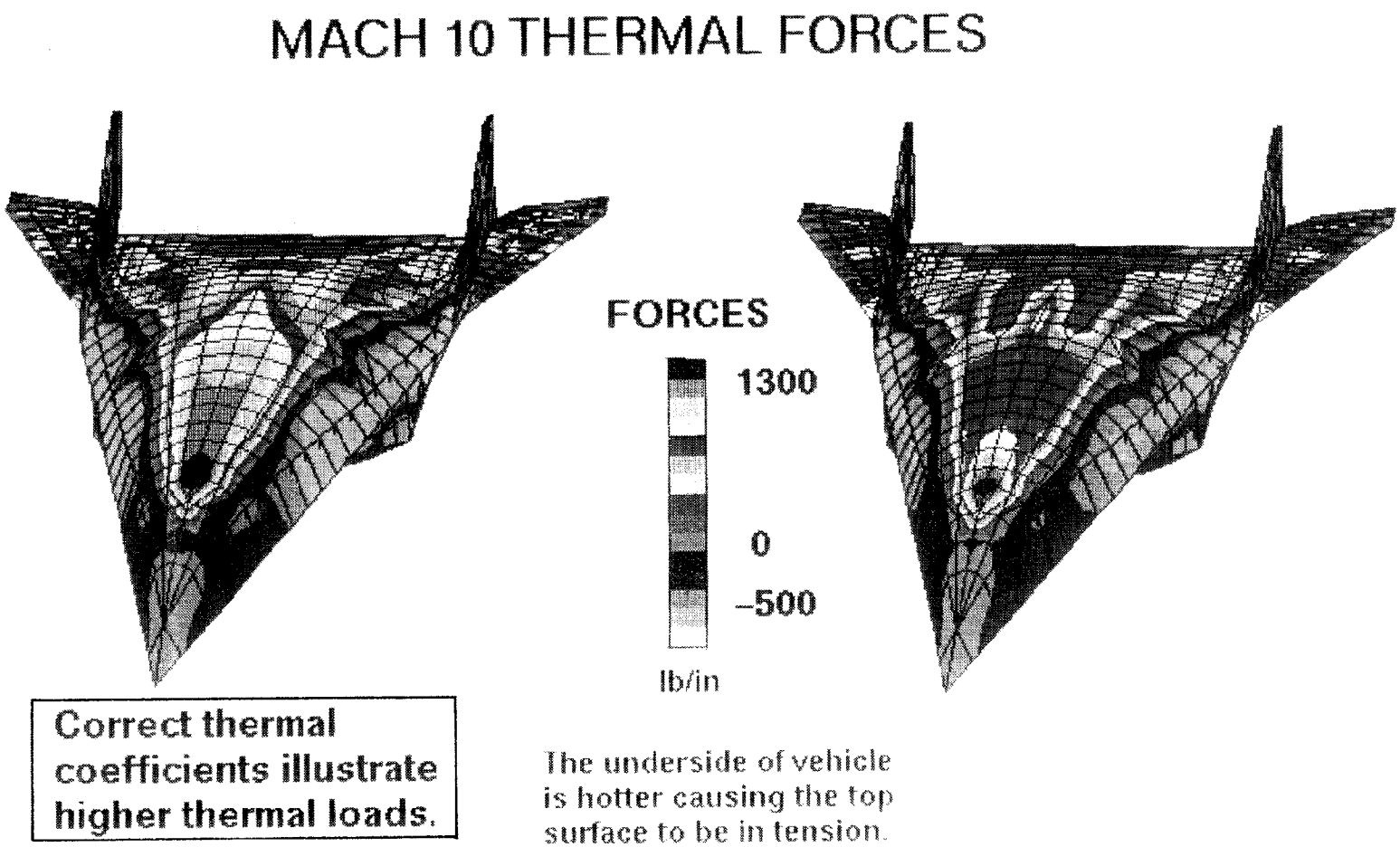


*Figure 10A Comparison of analytically predicted Mach 10 thermal forces of an aero-space plane.*

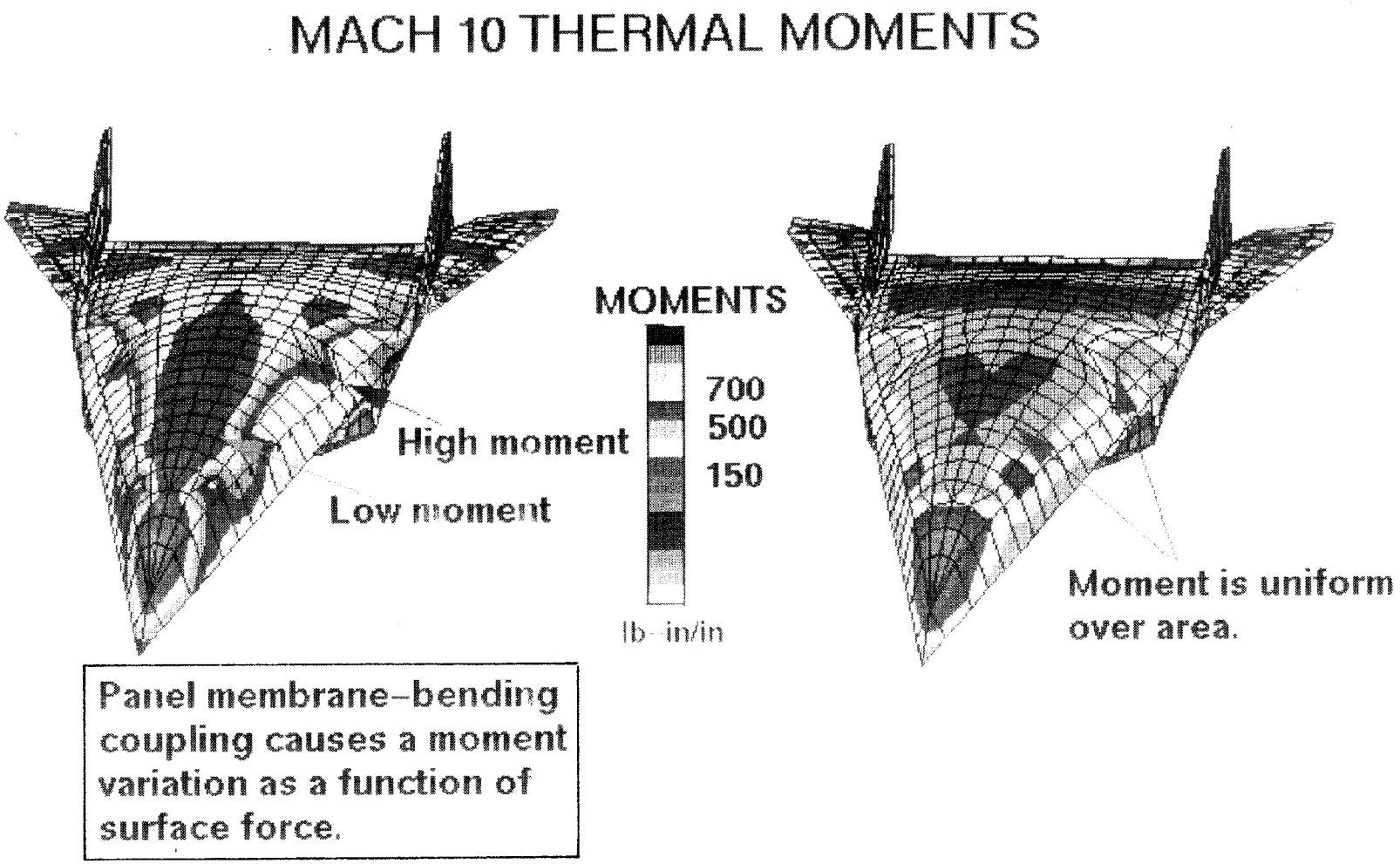


*Figure 10B Comparison of analytically predicted Mach 10 thermal moments of an aero-space plane.*